European Polymer Journal 203 (2024) 112694

Contents lists available at ScienceDirect

European Polymer Journal

journal homepage: www.elsevier.com/locate/europolj

Preparation of poly(oxanorbornene) based single and double-folding polymers via nucleophilic aromatic substitution reaction

Burcu Alkan [a,b], Binnur Aydogan Temel [c], Hakan Durmaz [a,*], Gokhan Temel [d,*]

[a] Department of Chemistry, Istanbul Technical University, 34469 Maslak, Istanbul, Turkey
[b] Yalova Vocational School, University of Yalova, 77200 Yalova, Turkey
[c] Department of Pharmaceutical Chemistry, Faculty of Pharmacy, Bezmialem Vakif University, Fatih, Istanbul 34093, Turkey
[d] Department of Polymer Material Engineering, Faculty of Engineering, Yalova University, Yalova 77200, Turkey

ARTICLE INFO

Keywords:
Single–chain nanoparticles
Cyanuric chloride
Soft nanoparticles
Ring-opening metathesis polymerization
Chain folding

ABSTRACT

A facile approach is introduced to prepare single-chain nanoparticles (SCNPs) utilizing intramolecular crosslinking based on nucleophilic aromatic substitution reaction. The linear polymeric precursor comprising dichlorotriazine (DCT) moiety as a reactive pendant group is synthesized via ring-opening metathesis polymerization (ROMP). The reactive chlorine atoms on DCT motifs are substituted with a dithiol nucleophile in varying degrees to yield individually intramolecularly crosslinked polymer nanoparticles. In addition, double-collapse and modification reactions are exploited through the substitution reaction from the remaining unreacted chlorine atoms. A significant reduction in hydrodynamic volumes of the corresponding SCNPs is observed compared to their linear analogues. The obtained nanoparticles are characterized by size exclusion chromatography (SEC), proton nuclear magnetic resonance spectroscopy (^{1}H NMR), diffusion-ordered spectroscopy (DOSY), dynamic light scattering (DLS), and transmission electron microscopy (TEM) techniques.

1. Introduction

The development of polymeric nanoparticles has drawn considerable attention over the past years due to their exceptional properties and diverse range of applications in the field of nanoscience [1–3]. Intramolecular chain folding strategy has been introduced to prepare single-chain nanoparticles (SCNPs), a novel class of well-defined and nanometer-sized polymeric nanoparticles [4–8]. Intramolecular interactions are performed through the crosslinking of the functional groups along the side-chain of an individual polymer chain or by utilizing the reactive bifunctional molecules to generate SCNPs [9–11]. In addition, sufficiently dilute polymer solutions are required to minimize the interchain interactions, thus resulting in a change in conformation from an expanded coil to a collapsed particle [12,13]. Not only developing the efficient approaches to synthesize the SCNPs but also controlling the size and the structure of the final product gain importance for practical applications.

The self-collapsing of an individual polymer chain by means of covalent, non-covalent, or dynamic covalent intramolecular interactions has been considered an appealing approach for the generation of a folded-chain structure [14–16]. Among all crosslinking strategies, covalent interactions such as photochemical reactions [17–21], Diels-Alder reaction [22], and click chemistry [23,24] have gained particular interest in generating self-crosslinked nanoparticles.

1,3,5-Triazine derivatives, six-membered heterocycles comprising three nitrogen atoms, are well-known organic building blocks and have gained considerable interest due to their chemical, industrial, and biological importance [25–28]. Among them, cyanuric chloride (2,4,6-trichloro-1,3,5-triazine) (TCT) has become privileged due to the high reactivity of its chlorine atoms towards a wide range of nucleophiles [29,30]. Also, 2,4,6-mono-, di- and tri-substituted triazines can be accessed *via* TCT in a one-pot or sequential manner, depending on the reaction conditions (e.g., temperature, catalyst), enabling versatility and selectivity. Thus, TCT has been widely employed as a reactive and versatile intermediate in (bio)organic chemistry [30]. This compound has also found applications at the macromolecular level to construct various polymer architectures such as monomer synthesis [31,32], dendrimer [33–36], linear/non-linear polymer synthesis [37–40], and polymer end-group/side-chain functionalization [41–43].

In this study, we aimed to adopt this robust and operationally simple nucleophilic aromatic substitution reaction to the preparation of SCNPs. For this purpose, an oxanorbornene monomer possessing a

* Corresponding author.
E-mail addresses: durmazh@itu.edu.tr (H. Durmaz), gtemel@yalova.edu.tr (G. Temel).

https://doi.org/10.1016/j.eurpolymj.2023.112694
Received 10 October 2023; Received in revised form 11 December 2023; Accepted 14 December 2023
Available online 16 December 2023
0014-3057/© 2023 Elsevier Ltd. All rights reserved.

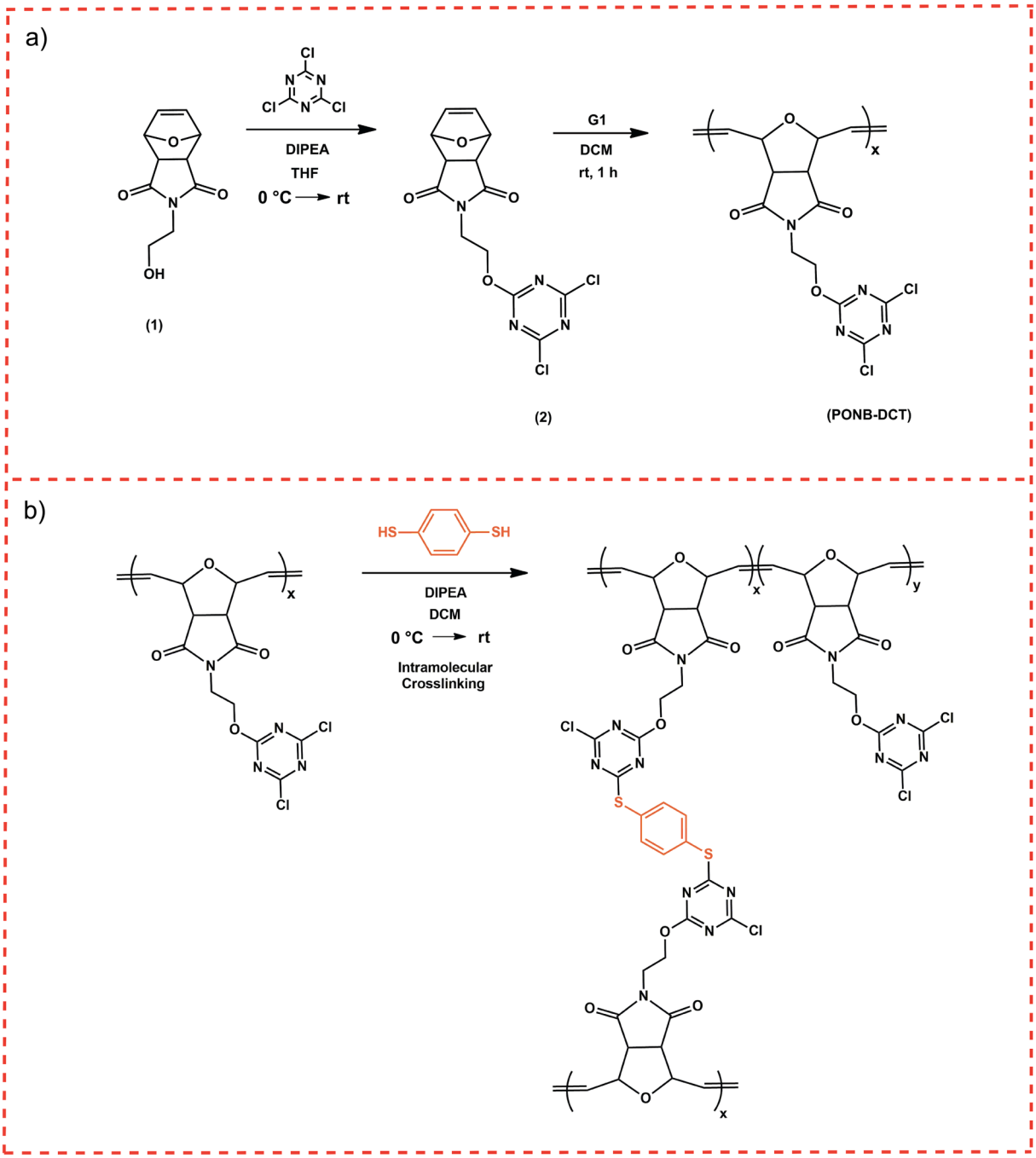

Scheme 1. a) Preparation of precursor polymer (PONB-DCT) via ROMP and b) intramolecular crosslinking using BDT.

dichlorotriazine (DCT) unit was synthesized and then polymerized *via* ring-opening metathesis polymerization (ROMP) to prepare a polymer precursor comprising the DCT moiety in the pendant group. Intramolecular crosslinking was successfully achieved by introducing varying degrees of the crosslinker benzene-1,4-dithiol (BDT) nucleophile. Furthermore, since unreacted chlorine atoms were still present along the backbone, double-folding and model modification studies were also performed on the prepared polymeric nanoparticles (Scheme 1).

2. Experimental

2.1. Materials

Furan (99 %, Sigma-Aldrich), maleic anhydride (99 %, Sigma-Aldrich), ethanolamine (99 %, Sigma-Aldrich), 2,4,6-trichloro-1,3,5-triazine (TCT, 99 %, Sigma-Aldrich), *N*,*N*-diisopropylethylamine (DIPEA, 99 %, Sigma-Aldrich), benzene-1,4-dithiol (BDT, 99 %, Sigma-Aldrich), 4,4′-thiobisbenzenethiol (99 %, Sigma-Aldrich), first-generation Grubbs catalyst (G1) ($(PCy_3)_2(Cl)_2RuCHPh$ (99 %, Sigma-Aldrich), 2-napthalenethiol (99 %, Sigma-Aldrich), toluene (99.8 %, Sigma-Aldrich) was used as received. Tetrahydrofuran (THF), dichloromethane (DCM), and diethyl ether were of anhydrous grade and used without further purification. Methanol (MeOH) was of reagent grade and used as received.

2.2. Instrumentation

^{1}H NMR (500 MHz) spectra were recorded using an Agilent VNMRS

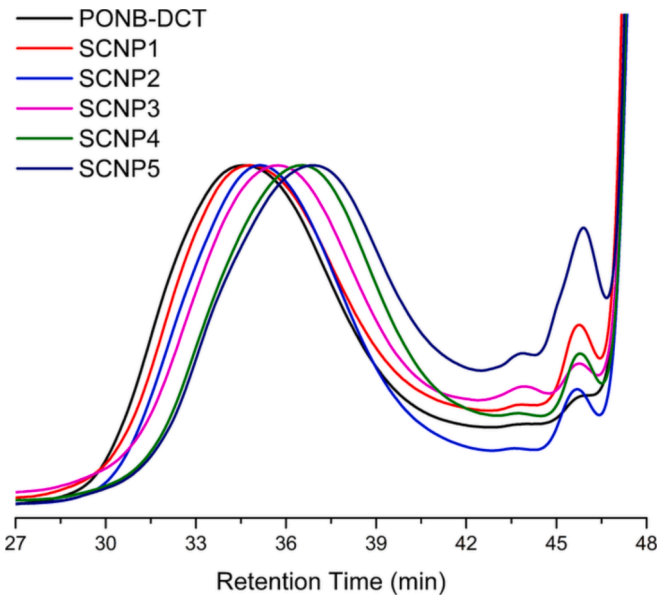

Fig. 1. Overlaid SEC traces of precursor polymer (PONB-DCT) and its single-chain nanoparticles (SCNP1–5) in THF at 30 °C.

Table 1
Characterization details of precursor polymer and the resulting SCNPs.

Entry	BDT[a] (equivalent)	M_n[b] (kDa)	M_w[b] (kDa)	$Đ$[b]	D_H[c] (nm)
PONB-DCT	–	15.5	26.5	1.71	10.29
SCNP1	0.1	14.4	24.3	1.68	7.38
SCNP2	0.2	14.3	21.6	1.52	7.24
SCNP3	0.3	13.2	19.9	1.50	7.17
SCNP4	0.4	11.4	16.7	1.46	6.82
SCNP5	0.5	11.0	15.9	1.43	6.30
SCNP2-DF	0.2[d]	6.1	9.9	1.61	7.67
SCNP3-DF	0.1[d]	8.7	13.6	1.56	7.82
SCNP2-M[e]	–	15.8	25.1	1.58	nd

[a] Per repeating unit in the precursor polymer.
[b] Determined by SEC calibrated based on linear PS standards in THF at 30 °C.
[c] Particle size determined by DLS.
[d] 4,4′-Thiobisbenzenethiol was used as crosslinker.
[e] Post-modification of SCNP2 with 2-napthalenethiol.

500 instrument in $CDCl_3$. Diffusion Ordered Spectroscopy (DOSY) measurements were performed at 298 K on a Bruker 500 Avance III HD Spectrometer operating at a frequency of 500.13 MHz and equipped with a z-gradient bbfo/5 mm tuneable "SmartProbe"™ probe and a GRASP II gradient spectroscopy accessory providing a maximum gradient output of 53.5 G cm^{-1} (5.35 G cm A^{-1}). Samples were dissolved in $CDCl_3$, and DOSY spectra were obtained using the ledbpgp2s pulse program from the Bruker TopSpin software. A relaxation delay of 12 s was employed along with a diffusion time (large delta) of 100 ms, a longitudinal eddy current delay (LED) of 5 ms, and a bipolar gradient pulse of 3 ms. The gradient strength was linearly incremented from 2 % at 0.96 G to 95 % at 45.7 G in 64 steps. The obtained data were processed using TopSpin 4.2.0 and Dynamics Center 2.5.6. Hydrodynamic diameters DH were calculated using the Stokes–Einstein equation. The size-exclusion chromatography (SEC) measurements were carried out with an Agilent instrument (Model 1100) with a pump, refractive index and UV detectors and four Waters Styragel columns (HR 5E, HR 4E, HR 3, HR 2), (4.6 mm internal diameter, 300 mm length, packed with 5 μm particles). The effective molecular weight ranges of columns were 2000–4,000,000, 50–100,000, 500–30,000, and 500–20,000 g/mol, respectively. THF was used as an eluent at a flow rate of 0.3 mL/min at 30 °C, and 2,6-di-*tert*-butyl-4-methylphenol was used as an internal standard. The number-average molecular weight (M_n), weight-average molecular weight (M_w), and dispersity ($Đ$) of the polymers were calculated based on narrow linear polystyrene (PS) standards (Polymer Laboratories). The morphology of nanostructures was analyzed by a JEOL 1220 JEM transmission electron microscope (TEM). HR-TEM samples were prepared by drop coating a dilute solution of the sample (in THF c = 0.01 mg mL^{-1}) on a holey carbon-coated copper grid. Particle size distributions were determined using dynamic light scattering (DLS) in THF dispersions using a Malvern Nano ZSP instrument. A detection angle of 173° (backscattering) was used for the measurements. Mean values of the number weighted diameter were calculated from five measurements in each case. HRMS analysis was carried out by Thermo Fisher Scientific LC-HRMS Thermo Q Exactive Spectrometer. Differential scanning calorimetry (DSC) measurements were carried out on a TA instrument (Q1000 series) under a nitrogen atmosphere in the temperature range from 0 °C to 150 °C at a scan rate of 10 °C/min. All data were collected from a second heating cycle, and the glass transition temperatures (T_g) were determined from the midpoint of calculated onset and endset temperatures of the glass transition region of the related DSC curve.

2.3. Synthetic procedures

4-(2-Hydroxyethyl)-10-oxa-4-aza-tricyclo[5.2.1.02,6]dec-8-ene-3,5-dione **(1)** was synthesized according to the published procedure [44].

2.3.1. Synthesis of dichlorotriazine-functionalized oxanorbornene monomer (2)

TCT (14.1 g, 0.076 mol) was added to a stirred solution of **1** (8 g, 0.038 mol) and DIPEA (13.3 mL, 0.076 mol) in THF at 0 °C. The solution was stirred at 0 °C for 3 h, warmed to room temperature, and stirred for an additional 16 h. At the end of this period, the solvent was removed under reduced pressure. The residue was dissolved in DCM, and the resulting salt was removed by filtration before extraction with water (2 × 100 mL). The collected organic layers were dried over anhydrous Na_2SO_4, and the solvent was removed under reduced pressure. The residue was washed with the mixture of DCM:diethyl ether (1:10) to give the product as a pale yellow powder (yield = 5.19 g, 38 %). ^{1}H NMR ($CDCl_3$, δ): 6.51 (s, 2H, C*H*=C*H*, bridge protons), 5.24 (s, 2H, C*H*O, bridge-head protons), 4.68 (t, 2H, NCH_2CH_2O), 3.94 (t, 2H, NCH_2CH_2O), 2.88 (s, 2H, C*H*-C*H*, bridge protons). HRMS (+ESI): $C_{13}H_{10}Cl_2N_4O_4$ calculated 357.15 $[M + H]^+$, found: 357.014.

2.3.2. Synthesis of poly(oxanorbornene dichlorotriazine) (PONB-DCT) via ROMP

2 (3 g, 8.4 mmol) was placed in a Schlenk tube and dissolved in 13 mL of anhydrous DCM. The first-generation Grubbs catalyst (G1) (0.138 g, 0.168 mmol) was dissolved in 2 mL of anhydrous DCM and added to the monomer solution. The reaction mixture was degassed by two freeze–pump–thaw (FPT) cycles, left in a vacuum, and stirred for 1 h at room temperature. At the end of this period, butyl vinyl ether (1.5 mL) was added to quench the polymerization, and the reaction was allowed to stir for an additional 30 min. Finally, the polymerization mixture was precipitated in diethyl ether, and the residual solvent was removed by decantation. The dissolution-precipitation process (DCM-diethyl ether) was repeated to yield the polymer as a pale yellow powder (yield = 2.7 g, 90 %). ^{1}H NMR ($CDCl_3$, δ): 6.05–5.79 (br, 2H, C*H*=C*H*), 4.99–4.49 (br, 4H, C*H*O and NCH_2CH_2O), 3.94 (br, 2H, NCH_2CH_2O), 3.41 (br, 2H, C*H*-C*H*).

2.3.3. General procedure for synthesis of single-chain nanoparticles (SCNPs): synthesis of SCNP1

PONB-DCT (0.2 g, 0.56 mmol) was dissolved in 180 mL of DCM and stirred at 0 °C for 1 h, then DIPEA (19.5 μL, 0.112 mmol) was added to this polymer solution at this temperature. Next, BDT (7.96 mg, 0.056 mmol) was dissolved in 20 mL of DCM and added dropwise with a

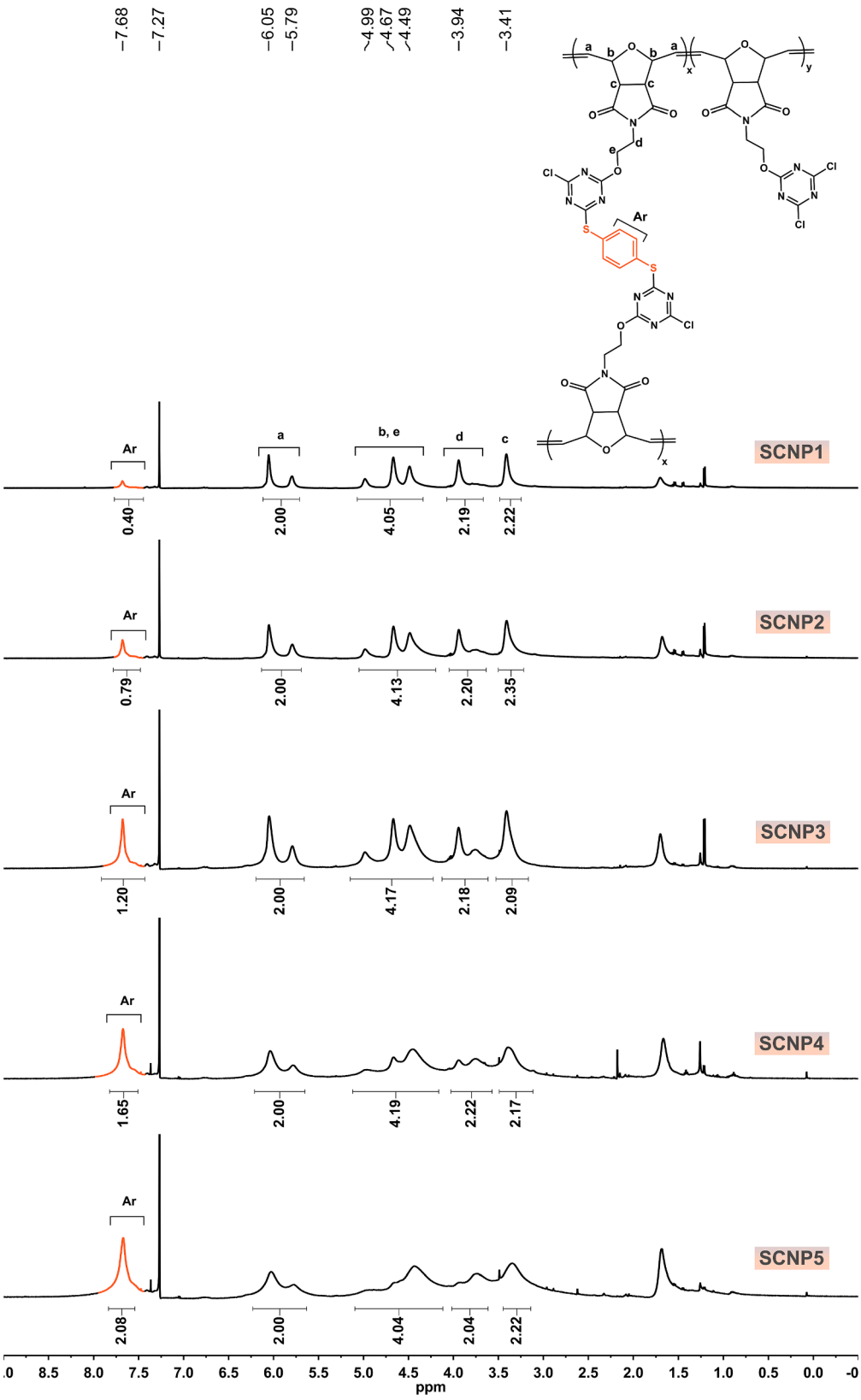

Fig. 2. ^{1}H NMR spectra of the resulting SCNPs in $CDCl_3$ (500 MHz).

dropping funnel to the reaction flask over 10 min with stirring. Afterward, the mixture was allowed to stir at 0 ℃ for 3 h, warmed to room temperature, and stirred for an additional 16 h. At the end of this period, the solvent was evaporated at room temperature, and the obtained SCNPs were precipitated in excess MeOH, filtered, and dried in a vacuum oven at room temperature for 24 h (yield = 114 mg). ^{1}H NMR ($CDCl_3$, δ): 7.68 (br, 4H, Ar*H*), 6.05–5.80 (br, 2H, C*H*═C*H*,), 4.99–4.49 (br, 4H, C*H*O and NCH$_2$C*H*$_2$O), 3.94–3.78 (br, 2H, NC*H*$_2$CH$_2$O), 3.41 (br,

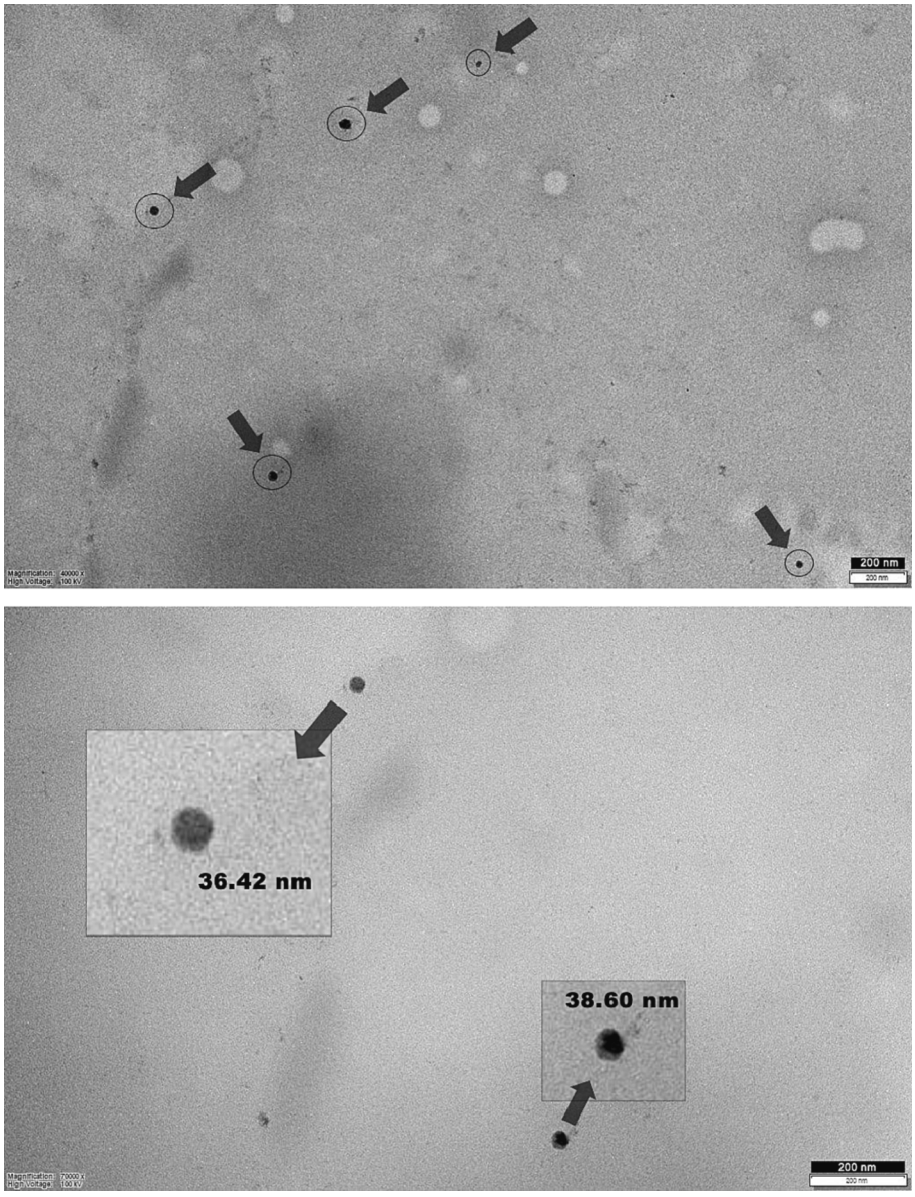

Fig. 3. TEM images of SCNP3. The scale bars show 200 nm.

2H, C*H*-C*H*). The same synthetic route was followed for the other SCNPs (SCNP2-5). The details can be found in the supporting information.

2.3.4. Double-folding reaction using SCNP2 (SCNP2-DF)

SCNP2 (0.1 g, 0.259 mmol) was dissolved in 80 mL of DCM and stirred at 0 ℃ for 1 h, then DIPEA (18.06 μL, 0.104 mmol) was added to this polymer solution at this temperature. Next, 4,4′-thiobisbenzenethiol (13 mg, 0.052 mmol) was dissolved in 20 mL of DCM and added dropwise with a dropping funnel to the reaction flask over 10 min with stirring. Afterward, the mixture was allowed to stir at 0 ℃ for 3 h, warmed to room temperature, and stirred for an additional 16 h. At the end of this period, the solvent was evaporated at room temperature, and the obtained SCNPs were precipitated in excess MeOH, filtered, and dried in a vacuum oven at room temperature for 24 h (yield = 78 mg). ^{1}H NMR ($CDCl_3$, δ): 7.68–7.42 (br, 12H, Ar*H*), 6.05–5.577 (br, 2H, C*H*═C*H*), 5.01–4.39 (br, 4H, C*H*O and NCH_2CH_2O), 3.94–3.75 (br, 2H, NCH_2CH_2O), 3.39 (br, 2H, C*H*-C*H*). The synthetic details for SCNP3-DF can be found in the supporting information.

2.3.5. Post-modification of SCNP2 (SCNP2-M)

SCNP2 (0.120 g, 0.311 mmol) was dissolved in 4 mL of DCM and stirred at 0 ℃ for 1 h. DIPEA (65 μL, 0.373 mmol) and 2-napthalenethiol (30 mg, 1.86 mmol) were added to the reaction medium, respectively. The mixture was allowed to stir at 0 ℃ for 3 h, then warmed to room temperature and stirred for an additional 16 h. At the end of this period, the resulting product (SCNP2-M) was precipitated in excess MeOH, filtered, and dried in a vacuum oven at room temperature for 24 h (yield = 110 mg). ^{1}H NMR ($CDCl_3$, δ): 8.03–7.52 (br, 12H, Ar*H*), 6.01–5.75 (br, 2H, C*H*═C*H*), 4.92–4.32 (br, 4H, C*H*O and NCH_2CH_2O), 3.64 (br, 2H, NCH_2CH_2O), 3.29 (br, 2H, C*H*-C*H*).

3. Results and discussion

Ring-opening metathesis polymerization (ROMP) and intramolecular crosslinking processes were combined in order to achieve single and double-folding/collapse polymer nanoparticles (SCNP and SCNP–DF). The precursor polymer was synthesized *via* conventional ROMP procedure using the first-generation Grubbs catalyst (G1) due to the fast initiation ability of the catalyst and high polymer yield at the end

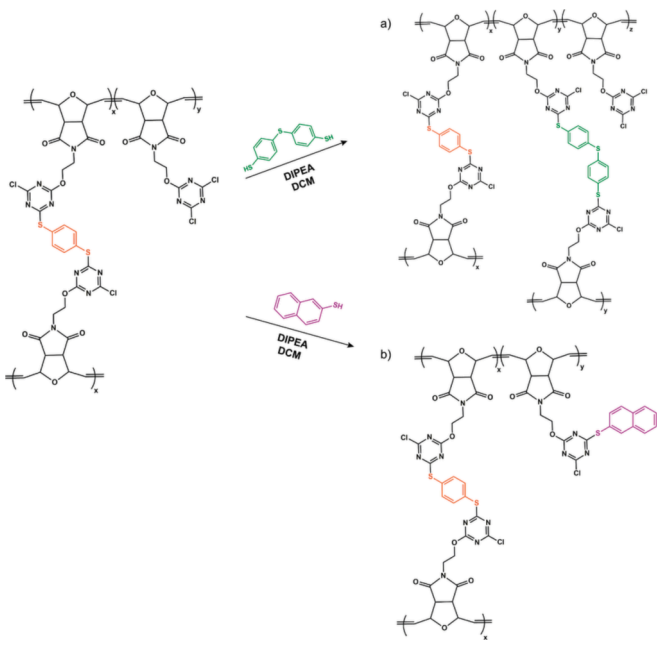

Scheme 2. a) Synthetic strategy for the double-folding process and b) modification of SCNP2 with 2-napthalenethiol.

of the short reaction period. First, to gain the desired polymer architecture, hydroxyl functionalized oxanorbornene monomer (**1**) was prepared according to a published procedure [44]. Subsequently, the resulting product was transformed into a DCT-functional oxanorbornene monomer (**2**), which was used in ROMP to obtain the precursor polymer (Scheme 1). The structure of **2** was analyzed by ^{1}H NMR spectroscopy. In addition to all bridge and bridge-head protons, methylene protons next to O and N were detected at 4.68 and 3.94 ppm, respectively, and the integral area ratios of these protons to the rest of the protons in the structure were in full agreement, indicating highly pure compound (Fig. S1). Next, the ROMP of **2** was performed at room temperature using the ratio of **2**/catalyst = 50, resulting in PONB-DCT in a high isolated yield (90 %). Fig. S2 represents the ^{1}H NMR spectrum of the polymer, showing all expected signals regarding the polymer. It should be noted here that the norbornene analogue of this monomer was synthesized previously and polymerized by ROMP, and the obtained polymer was used as a coupling reagent in various organic reactions. However, no data regarding the molecular weight and dispersity values for the obtained polymer was reported [45].

After the polymerization step, nucleophilic aromatic substitution methodology was employed to carry out the folding procedure of PONB-DCT and BDT in a dilute regime (c = 1.0 mg mL^{-1}). Berda group synthesized similar types of polymers with spacer units, but they reported that longer carbon spacers could not change intramolecular crosslinking efficiency [46]. Therefore, we preferred a two-carbon long spacer between the polymer backbone and the DCT unit. Folding reactions were performed following similar procedures reported by the Sumerlin group [41,42]. Also, a gradual increase was aimed in the amount of crosslinker BDT from 0.1 to 0.5 equivalents per repeating unit of the polymer, and DIPEA (Hünig's base) was used as a base in the reactions to facilitate the attack of thiols on chlorine atoms in the polymer side-chain. It is worth noting that the crosslinker (i.e., BDT) was purposely chosen to be aromatic due to its high acidity, which can favorably influence the efficiency of the substitution reaction in the presence of DIPEA and also because of its distinctive aromatic signals (Fig. 2) that allow reaction efficiencies to be easily monitored by NMR.

SEC analyses verified the formation of each SCNP, which exhibited a shift to longer retention time compared to their linear precursor and a decrease in particle size due to their more compact architecture. Also, no shoulders or tails were observed in the SEC traces of the nanoparticles, indicating smooth reactions (Fig. 1). All SEC and DLS characterization data of the precursor polymer and SCNPs are tabulated in Table 1. According to the SEC results, the M_n and $Đ$ values of PONB-DCT were found to be 15.5 kDa and 1.71, respectively. Additionally, the size of the polymer was detected as 10.29 nm by DLS (Fig. S7). Table 1 results show that all nanoparticles have lower M_n and M_w values and narrower polydispersity indexes than the parent polymer due to the reduction observed in particle sizes and the coil-to-globe transition. Besides, the amount of crosslinker directly affects the molecular weight results and particle sizes of the resulting nanoparticles; SCNP5 exhibits the most compact structure for the first folding process (6.30 nm) (Fig. S7).

The overlay of ^{1}H NMR spectra of SCNPs obtained using different amounts of crosslinker is given in Fig. 2. The integral values of the peaks

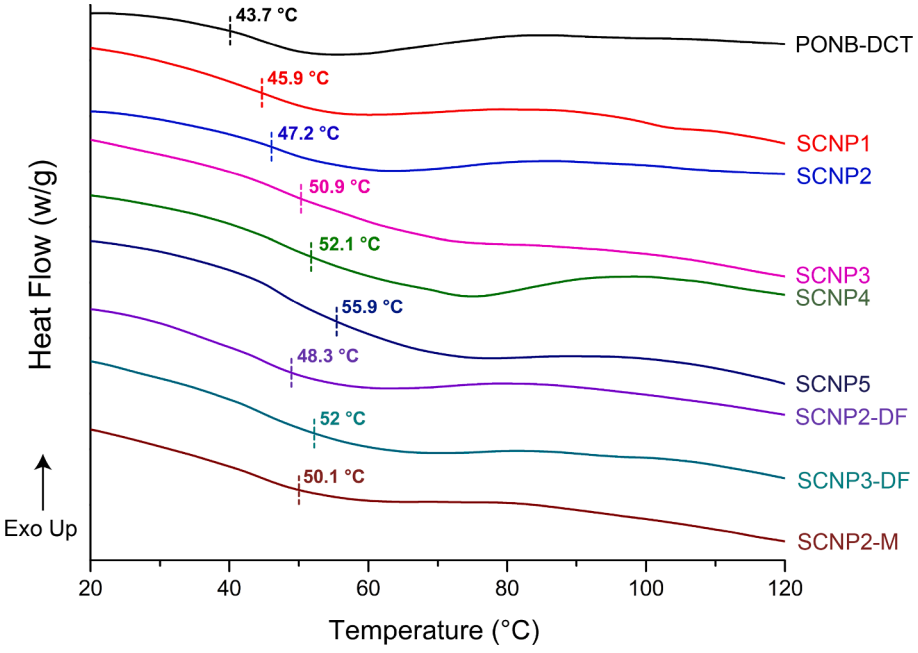

Fig. 4. DSC curves of linear precursor and SCNPs.

in the spectra are determined so that the C*H*═C*H* (2H) main chain protons at 6.05–5.79 ppm are 2. As can be seen in these spectra, all the integral ratios of the aromatic protons at 7.68 ppm were found to be in good agreement with the feeding ratio of the crosslinking agent. For instance, when 0.1 equivalent BDT was utilized per repeating unit, the integral ratio of the aromatic protons was found to be 0.4 for SCNP1. Likewise, when the amount of crosslinking agent was increased from 0.2 to 0.5 equivalents, the integral ratios of the aromatic protons were found to be 4 times higher than the feeding ratios, as expected. It should also be noted here that increasing the amount of BDT leads to broader signals, possibly indicating more compact structures.

To acquire more insight, DOSY NMR measurements were performed in $CDCl_3$ to determine the hydrodynamic diameter of the precursor polymer and polymeric nanoparticles. The Stokes–Einstein equation was used to calculate the hydrodynamic diameter of nanoparticles (see supporting information). A hydrodynamic diameter of 3.35 nm was calculated for the precursor polymer, whereas size reduction was observed for SCNP1 = 3.31 nm and SCNP3 = 3.14 nm. Slightly higher diffusion coefficients were obtained for SCNPs compared to the precursor polymer owing to their smaller sizes (Figs. S8–10). Furthermore, the hydrodynamic diameter of SCNPs decreased with the increased amount of crosslinker. Although a slight size reduction was obtained from DOSY experiments, they further supported the DLS measurements.

While DLS measurements of achieved SCNPs emphasize sub-10 nm particle size, transmission electron microscopy (TEM) images exhibit that polymer nanoparticles are prone to form larger spheres resulting from chain aggregation (Fig. 3). The nanoparticles have diameters in the range of 30–40 nm, which are much larger than the typical sizes of SCNPs reported (10–20 nm) [21,47]. This trend can be explained by solvent evaporation after casting on a copper grid, and nanoparticles appear to tend to coalesce during the drying process. Besides, coil-to-globe transition was easily detected by TEM results.

The versatility of the newly developed nucleophilic aromatic substitution strategy was also exploited for both double-folding and post-modification reactions via unreacted DCT units (Scheme 2). In the double-folding study, SCNP2 and SCNP3 were used as starting nanoparticles in the presence of a different crosslinker, 4,4′-thiobisbenzenethiol, to obtain double-folded nanoparticles SCNP2-DF and SCNP3-DF (see Table 1). According to molecular weight results, double-folded nanoparticles showed a dramatic decrease compared to their parent analogues. On the other hand, particle size values of double-folded products increased, and these results were attributed to unavoidable partial intermolecular crosslinking or interaction between nanoparticles during the second collapse process.

The success of the double-folding strategy was also confirmed by ^{1}H NMR analysis (Fig. S3). Since 60 % of the dichlorotriazine functionality remained unreacted in SCNP2, the maximum integral value of the aromatic protons was expected to be 2.4 when 33 % of the unreacted dichlorotriazine units were substituted with 4,4′-thiobisbenzenethiol via nucleophilic aromatic substitution reaction. Comparing the integral values of aromatic protons at 7.66–7.42 ppm with the integral values of C*H*═C*H* main chain protons at 6.05–5.79 ppm gave a result of 2.39, suggesting quantitative efficiency. Similar calculations were made for SCNP3-DF, and quantitative substitution efficiency was also found for this nanoparticle. Besides, double-folded products exhibit a distinct shift to longer retention times compared to their single-folded analogues based on SEC traces (Fig. S4).

Lastly, an attempt was made to modify a representative SCNP. To this end, a reaction was carried out between SCNP2 and 2-napthalenethiol, and all unreacted chlorine atoms in the nanoparticle (the remaining 60 %) were aimed to react. The modified nanoparticle (SCNP2-M) was characterized by ^{1}H NMR, where the integral area value of all aromatic protons at 8.05–7.18 ppm (~5H) perfectly matches with the above-mentioned main chain protons (2H), indicating the complete incorporation of the model thiol compound into the polymeric nanoparticle (Fig. S5). Moreover, since a monofunctional thiol was utilized in the reaction, a slight increment was observed in the M_n value of the resulting modified nanoparticle, from 14.3 kDa to 15.8 kDa, as expected (Fig. S6).

To gain more detailed information, the thermal properties of the precursor and folded polymers were determined by differential scanning calorimetry (DSC) analyses (Fig. 4). The loss of chain flexibility of nanoparticles is further evidence of the formation of crosslinked polymer chains. According to thermal test results, all single-folded polymers (SCNP1-5) reveal higher T_g values compared to the parent polymer due to the decrease of chain mobility as expected. Besides, T_g values of double-folded products increased proportionally with crosslinking degree and rigid aromatic content of the second crosslinker. 2-Napthalenethiol functionalized nanoparticle (SCNP2-M) showed a higher glass transition temperature (T_g = 50.1 °C) compared to its precursor SCNP2 (T_g = 47.2 °C) as well.

4. Conclusion

We have demonstrated here that pendant DCT units are able to effectively react with aromatic dithiol compounds in a dilute solvent medium to achieve intramolecularly crosslinked polymeric architectures. Characterization techniques confirmed that the presented route is efficient for single and double-collapse polymer syntheses. Also, the rest of the free chlorine atoms in the pendant DCT groups are still active for post-functionalization processes. Utilization of the corresponding nucleophilic aromatic substitution technique is a versatile tool for the synthesis and post-functionalization of novel soft nanoparticles. Overall, nucleophilic aromatic substitution strategy and other chemistries can be combined to develop new attractive nanostructures and applications in future works.

CRediT authorship contribution statement

Burcu Alkan: Data curation, Investigation, Methodology, Validation, Writing - original draft, Writing - review & editing, Software. **Binnur Aydogan Temel:** Software, Investigation, Writing - review & editing. **Hakan Durmaz:** Conceptualization, Data curation, Funding acquisition, Investigation, Methodology, Supervision, Validation, Writing - original draft, Writing - review & editing. **Gokhan Temel:** Conceptualization, Data curation, Funding acquisition, Conceptualization, Data curation, Funding acquisition, Investigation, Methodology, Supervision, Validation, Writing - original draft, Writing - review & editing.

Declaration of competing interest

The authors declare that they have no known competing financial interests or personal relationships that could have appeared to influence the work reported in this paper.

Data availability

Data will be made available on request.

Acknowledgements

This work was supported by the Scientific Research Projects Departments of Istanbul Technical University (ITU BAP Project Number: TDK-2023-44655). B. A. T. acknowledges the resources and support from the Drug Application and Research Center (ILMER) at Bezmialem Vakif University.

Appendix A. Supplementary data

Supplementary data to this article can be found online at https://doi.org/10.1016/j.eurpolymj.2023.112694.

References

[1] G. Li, F. Tao, L. Wang, Y. Li, R. Bai, A facile strategy for preparation of single-chain polymeric nanoparticles by intramolecular photo-crosslinking of azide polymers, Polymer 55 (16) (2014) 3696–3702.

[2] E.H.H. Wong, S.J. Lam, E. Nam, G.G. Qiao, Biocompatible single-chain polymeric nanoparticles via organo-catalyzed ring-opening polymerization, ACS Macro Lett. 3 (6) (2014) 524–528.

[3] J.P. Rao, K.E. Geckeler, Polymer nanoparticles: Preparation techniques and size-control parameters, Prog. Polym. Sci. 36 (7) (2011) 887–913.

[4] O. Altintas, C. Barner-Kowollik, Single chain folding of synthetic polymers by covalent and non-covalent interactions: current status and future perspectives, Macromol. Rapid Commun. 33 (11) (2012) 958–971.

[5] M.A.M. Alqarni, C. Waldron, G. Yilmaz, C.R. Becer, Synthetic routes to single chain polymer nanoparticles (SCNPs): current status and perspectives, Macromol. Rapid Commun. 42 (11) (2021), 2100035.

[6] A. Nitti, R. Carfora, G. Assanelli, M. Notari, D. Pasini, Single-chain polymer nanoparticles for addressing morphologies and functions at the nanoscale: A review, ACS Appl. Nano Mater. 5 (10) (2022) 13985–13997.

[7] J. Nam, S. Kwon, Y.-G. Yu, H.-B. Seo, J.-S. Lee, W.B. Lee, Y. Kim, M. Seo, Folding of sequence-controlled graft copolymers to subdomain-defined single-chain nanoparticles, Macromolecules 54 (18) (2021) 8829–8838.

[8] C.H. Liu, L.D. Dugas, J.I. Bowman, T. Chidanguro, R.F. Storey, Y.C. Simon, Forcing single-chain nanoparticle collapse through hydrophobic solvent interactions in comb copolymers, Polym. Chem. 11 (2) (2020) 292–297.

[9] B. Alkan, O. Daglar, B. Aydogan Temel, H. Durmaz, G. Temel, Rapid synthesis of polyester based single-chain polymeric nanoparticles via an intra-molecular aza-Michael addition reaction, Polym. Chem. 13 (17) (2022) 2442–2449.

[10] S. Babaoglu, D.K. Balta, G. Temel, Synthesis of photoactive single-chain folded polymeric nanoparticles via combination of radical polymerization techniques and Menschutkin click chemistry, J. Polym. Sci., Part A: Polym. Chem. 55 (12) (2017) 1998–2003.

[11] I. Dashan, D.K. Balta, B.A. Temel, G. Temel, Preparation of single chain nanoparticles via photoinduced double collapse process, Macromol. Chem. Phys. 220 (10) (2019), 1900116.

[12] M. Gonzalez-Burgos, A. Latorre-Sanchez, J.A. Pomposo, Advances in single chain technology, Chem. Soc. Rev. 44 (17) (2015) 6122–6142.

[13] A.M. Hanlon, C.K. Lyon, E.B. Berda, What is next in single-chain nanoparticles? Macromolecules 49 (1) (2016) 2–14.

[14] S. Mavila, O. Eivgi, I. Berkovich, N.G. Lemcoff, Intramolecular cross-linking methodologies for the synthesis of polymer nanoparticles, Chem. Rev. 116 (3) (2016) 878–961.

[15] G. Yilmaz, V. Uzunova, R. Napier, C.R. Becer, Single-chain glycopolymer folding via host-guest interactions and its unprecedented effect on DC-SIGN binding, Biomacromolecules 19 (7) (2018) 3040–3047.

[16] Y. Shao, Z. Yang, Progress in polymer single-chain based hybrid nanoparticles, Prog. Polym. Sci. 133 (2022), 101593.

[17] C. Heiler, J.T. Offenloch, E. Blasco, C. Barner-Kowollik, Photochemically induced folding of single chain polymer nanoparticles in water, ACS Macro Lett. 6 (1) (2017) 56–61.

[18] J. Willenbacher, K.N.R. Wuest, J.O. Mueller, M. Kaupp, H.-A. Wagenknecht, C. Barner-Kowollik, Photochemical design of functional fluorescent single-chain nanoparticles, ACS Macro Lett. 3 (6) (2014) 574–579.

[19] M. Bilgi, D.K. Balta, B.A. Temel, G. Temel, Single-chain folding nanoparticles as carbon nanotube catchers, J. Polym. Sci., Part A: Polym. Chem. 56 (24) (2018) 2709–2714.

[20] P.G. Frank, B.T. Tuten, A. Prasher, D. Chao, E.B. Berda, Intra-chain photodimerization of pendant anthracene units as an efficient route to single-chain nanoparticle fabrication, Macromol. Rapid Commun. 35 (2) (2014) 249–253.

[21] D. Kilic, C. Pamukcu, D.K. Balta, B.A. Temel, G. Temel, Rapid synthesis of fluorescent single-chain nanoparticles via photoinduced step-growth polymerization of pendant carbazole units, Eur. Polym. J. (2020), 109469.

[22] A.M. Hanlon, I. Martin, E.R. Bright, J. Chouinard, K.J. Rodriguez, G.E. Patenotte, E. B. Berda, Exploring structural effects in single-chain “folding” mediated by intramolecular thermal Diels-Alder chemistry, Polym. Chem. 8 (34) (2017) 5120–5128.

[23] A. Sanchez-Sanchez, I. Perez-Baena, J.A. Pomposo, Advances in click chemistry for single-chain nanoparticle construction, Molecules 18 (3) (2013) 3339–3355.

[24] A. Sanchez-Sanchez, I. Asenjo-Sanz, L. Buruaga, J.A. Pomposo, Naked and self-clickable propargylic-decorated single-chain nanoparticle precursors via redox-initiated RAFT polymerization, Macromol. Rapid Commun. 33 (15) (2012) 1262–1267.

[25] K. Arya, A. Dandia, Synthesis and cytotoxic activity of trisubstituted-1,3,5-triazines, Bioorg. Med. Chem. Lett. 17 (12) (2007) 3298–3304.

[26] P. Singla, V. Luxami, K. Paul, Triazine as a promising scaffold for its versatile biological behavior, Eur. J. Med. Chem. 102 (2015) 39–57.

[27] M.E. Quirke, 1,3,5-Triazines, in: A.R. Katritzky, C.W. Rees (Eds.), Comprehensive Heterocyclic Chemistry, Pergamon, New York, NY, 1984, pp. 457–530.

[28] D. Bartholomew, 1,3,5-Triazines, in: A.J. Boulton (Ed.), Comprehensive Heterocyclic Chemistry II, Pergamon, Oxford, 1996, p. 575.

[29] D.A. Probst, P.R. Hanson, D.A. Barda, Cyanuric Chloride, Encyclopedia of Reagents for Organic Synthesis (EROS)2004.

[30] G. Blotny, Recent applications of 2,4,6-trichloro-1,3,5-triazine and its derivatives in organic synthesis, Tetrahedron 62 (41) (2006) 9507–9522.

[31] M. Ak, M.S. Ak, L. Toppare, Electrochemical properties of a new star-shaped pyrrole monomer and its electrochromic applications, Macromol. Chem. Phys. 207 (15) (2006) 1351–1358.

[32] M. Guzel, T. Soganci, E. Karatas, M. Ak, Donor-acceptor type super-structural triazine cored conducting polymer containing carbazole and quinoline for high-contrast electrochromic device, J. Electrochem. Soc. 165 (7) (2018) H316.

[33] M.B. Steffensen, E.E. Simanek, Chemoselective building blocks for dendrimers from relative reactivity data, Org. Lett. 5 (13) (2003) 2359–2361.

[34] M.B. Steffensen, E. Hollink, F. Kuschel, M. Bauer, E.E. Simanek, Dendrimers based on [1,3,5]-triazines, J. Polym. Sci., Part A: Polym. Chem. 44 (11) (2006) 3411–3433.

[35] S. Patra, B. Kozura, A.Y.T. Huang, A.E. Enciso, X. Sun, J.-T. Hsieh, C.-L. Kao, H.-T. Chen, E.E. Simanek, Dendrimers terminated with dichlorotriazine groups provide a route to compositional diversity, Org. Lett. 15 (15) (2013) 3808–3811.

[36] A.E. Enciso, Z.M. Abid, E.E. Simanek, Rapid, semi-automated convergent synthesis of low generation triazine dendrimers using microwave assisted reactions, Polym. Chem. 5 (16) (2014) 4635–4640.

[37] S. Kondo, T. Yamamoto, H. Kunisada, Y. Yuki, Aromatic nucleophilic substitution polymerization of dichloro-1,3,5-triazines with alkanedithiols, J. Macromol. Sci.: Part A – Chem. 27 (12) (1990) 1513–1528.

[38] S.M. Osman, S.N. Khattab, E.-S.-A. Aly, E.-R. Kenawy, A. El-Faham, 1,3,5-Triazine-based polymer: synthesis, characterization and application for immobilization of silver nanoparticles, J. Polym. Res. 24 (12) (2017) 231.

[39] S.K. Kundu, A. Bhaumik, A triazine-based porous organic polymer: a novel heterogeneous basic organocatalyst for facile one-pot synthesis of 2-amino-4H-chromenes, RSC Adv. 5 (41) (2015) 32730–32739.

[40] B. Nayak, A. Mukherjee, S. Basu, P. Bhanja, B.K. Jena, Metal-free triazine-based porous organic polymer-derived N-doped porous carbons as effective electrocatalysts for oxygen reduction reaction, ACS Appl. Energy Mater. 5 (12) (2022) 15899–15908.

[41] C.A. Figg, T. Kubo, B.S. Sumerlin, Efficient and chemoselective synthesis of ω, ω-heterodifunctional polymers, ACS Macro Lett. 4 (10) (2015) 1114–1118.

[42] T. Kubo, C.A. Figg, J.L. Swartz, W.L.A. Brooks, B.S. Sumerlin, Multifunctional homopolymers: postpolymerization modification via sequential nucleophilic aromatic substitution, Macromolecules 49 (6) (2016) 2077–2084.

[43] M. Sadeghi-Kiakhani, A.R. Tehrani-Bagha, S. Safapour, Enhanced anti-microbial, anti-creasing and dye absorption properties of cotton fabric treated with chitosan-cyanuric chloride hybrid, Cellulose 25 (1) (2018) 883–893.

[44] G. Mantovani, F. Lecolley, L. Tao, D.M. Haddleton, J. Clerx, J.J.L.M. Cornelissen, K. Velonia, Design and synthesis of N-maleimido-functionalized hydrophilic polymers via copper-mediated living radical polymerization: A suitable alternative to PEGylation chemistry, J. Am. Chem. Soc. 127 (9) (2005) 2966–2973.

[45] A. Rolfe, D.A. Probst, K.A. Volp, I. Omar, D.L. Flynn, P.R. Hanson, High-load, oligomeric dichlorotriazine: A versatile ROMP-derived reagent and scavenger, J. Org. Chem. 73 (22) (2008) 8785–8790.

[46] R. Chen, S.J. Benware, S.D. Cawthern, J.P. Cole, J.J. Lessard, I.M. Crawford-Eng, R. Saxena, E.B. Berda, Assessing structure/property relationships and synthetic protocols in the fabrication of poly(oxanorbornene imide) single-chain nanoparticles, Eur. Polym. J. 112 (2019) 206–213.

[47] I. Dashan, D.K. Balta, B.A. Temel, G. Temel, Preparation of single chain nanoparticles via photoinduced radical coupling process, Eur. Polym. J. 113 (2019) 183–191.